Issue 9, 2017

From the journal:
Analyst

Enhanced detection of quantum dots by the magnetohydrodynamic effect for electrochemical biosensing

Daniel Martín-Yerga,*[a] Pablo Fanjul-Bolado,[b] David Hernández-Santos[b] and Agustín Costa-García*[a]

Author affiliations

* Corresponding authors

[a] Departamento de Química Física y Analítica, Universidad de Oviedo, 33006 Oviedo, Spain
E-mail: martindaniel@uniovi.es, costa@uniovi.es
Tel: (+34) 985103486

[b] DropSens, S.L., Edificio CEEI, Parque Tecnológico de Asturias, 33428 Llanera, Spain

https://doi.org/10.1039/C7AN00086C

Enhanced detection of quantum dots by the magnetohydrodynamic effect for electrochemical biosensing

Daniel Martín-Yerga[1], Pablo Fanjul-Bolado[2], David Hernández-Santos[2], and Agustín Costa-García[1*]*

[1] Departamento de Química Física y Analítica**,** Universidad de Oviedo, 33006 Oviedo, Asturias, Spain.

[2] DropSens, S.L., Edificio CEEI, Parque Tecnológico de Asturias, 33428 Llanera, Asturias, Spain

* Corresponding authors: Dr. Daniel Martín Yerga, Prof. Dr. Agustín Costa-García

Departamento de Química Física y Analítica

Universidad de Oviedo

Julián Clavería 8, Oviedo 33006 (Spain)

E-mails: martindaniel@uniovi.es; costa@uniovi.es

Telephone: (+34) 985103486

ABSTRACT

In this work, we describe the use of a magnetoelectrochemical support for screen-printed electrodes to improve the anodic stripping voltammetry of cadmium due to the generated magnetohydrodynamic (MHD) effect. To create a significant MHD effect, Fe(III) was added at mM concentrations to the solution. The reduction of Fe(III) simultaneously with the cadmium deposition on the electrode surface allowed to produce a high cathodic current, which generated a large Lorentz force capable of causing a convective effect on the solution in presence of the magnetic field. This convective effect allowed to increase the mass transfer in the quiescent solution, enhancing the deposition of cadmium as observed by an increased stripping peak current. The optimized method was applied to the detection of CdSe/ZnS quantum dots (QDs) in solution. Using the magnetoelectrochemical support, we were able to detect extremely low concentrations of QDs, with a detection limit of 100 amol of QDs (in particle number). The great performance showed by this system was evaluated in biosensing applications. Firstly, the detection of biotin was carried out using a competitive bioassay between biotin and QDs-labelled biotin, obtaining good analytical results (0.6×10^{-10} M as limit of detection). Then, the magnetoelectrochemical support was tested in a more complex biosensor for the determination of anti-transglutaminase IgA antibodies, a celiac disease biomarker. This work shows that the improvement in the metal electrodeposition by the MHD effect can be used successfully and with great performance for the development of disposable electrochemical biosensors using screen-printed electrodes.

KEYWORDS: magnetoelectrochemistry; magnetohydrodynamics; biosensing; quantum dots; celiac disease

1. INTRODUCTION

The application of magnetic fields in electrochemical cells can be used in different approaches. One of these approaches is the commonly called magnetoelectrochemistry[1], which is used to change the electrochemical behaviour of redox species, mainly by producing a change of the mass transfer in the electrochemical cell. Magnetoelectrochemical studies have been applied to improve mass transfer to electrodes by a magnetic gradient force[2] generated at electrodes modified with magnetic particles[3]. However, magnetoelectrochemistry is mainly used by taking advantage of the effect generated by the Lorentz force[4]. When a magnetic field is applied to an electrochemical cell, the interaction between the current density and the magnetic field density induces a Lorentz force. The magnitude and direction of the Lorenz force is defined by the right-hand rule[5], according to the following equation:

$$\overrightarrow{F_L} = \vec{J}\, x\, \vec{B} \quad \textbf{(1)}$$

where F_L is the magnetic Lorentz force by unit volume of solution (N/m^3), J is the current density (A/m^2) and B is the magnetic field density (T). By this equation, it can be seen that higher magnetic fields or current densities induce greater Lorentz forces. Another aspect is apparent from this equation, since the magnitudes are vector: if the magnetic field and the current density are in a perpendicular direction, the Lorentz force is maximum, but if they are in a parallel direction, the Lorentz force is cancelled. This force will influence the solution of the electrochemical cell, generating a flow movement (increased mass transfer by forced convection). This effect, called magnetohydrodynamic (MHD) effect, can be particularly interesting to enhance mass transfer in micro-volume electrochemical cells that cannot be stirred mechanically. The MHD effect has been widely used for studying metal electrodeposition, in which high concentrations of the species to be electrodeposited are used, and have focused on the study of morphology[6], crystal microstructure of the electrodeposited film[7] or kinetics[8]. This convective effect has also been used to improve the detection of heavy metals using anodic stripping voltammetry (ASV). In this technique, the metal is preconcentrated on the electrode surface by electrodeposition, and the stripping signal (oxidation of

the deposited metal) is recorded. The stripping signal is proportional to the concentration of metal in solution. This technique is extremely sensitive because it allows to preconcentrate on the electrode surface improving the detection compared to species transported by diffusion to the electrode surface. Furthermore, if a magnetic field is applied while the reduction occurs (if a high current is flowing), a significant Lorentz force could be generated enhancing the ion transfer in solution due to the forced convection. Although the solution is not stirred during the metal electrodeposition, the ionic transport will be more effective, achieving a greater preconcentration on the electrode surface, and therefore, improving the detection. Fritsch et al. have published several works where they study the improvement of the detection of heavy metals such as cadmium or lead using the MHD effect. They observed that the effect of mercury, used to generate a thin-film on the electrode surface, was enough to improve the preconcentration in the presence of the magnetic field. However, the possibility to use less toxic species at higher concentrations such as Fe(III) was the most appropriate strategy for the detection of heavy metals in presence of magnetic fields, and the resulting species, Fe(II), was also soluble, avoiding interfering effects[9]. They also described that the use of benzoquinone may be interesting to generate a high cathodic current during the metal electrodeposition, as this species transfer two electrons[10]. The effect of different experimental parameters such as the magnetic field intensity, the volume of the solution, electrode size or detection technique was also studied[11,12]. Similar systems were used by other authors for the detection of mercury[13] and lead[14]. Other interesting applications of the convective effect generated by the Lorentz force in redox systems may be the possibility of pumping solutions in microfluidic devices without external pumps or without a channel to direct the flow[15]. Interestingly, pumping in microfluidic systems have been possible without redox species at high concentrations by using the transient portion of the current during a potential step[16] (i.e. the high current produced initially by the charging of the double layer). The use of the MHD effect to improve electrochemical applications appears to be very useful with numerous possibilities. However, as far as we are aware,

the use of this effect to enhance the detection in disposable electrochemical biosensors has not yet been described.

Quantum dots (QDs) are semiconductor nanocrystals being widely used for several applications due to their special optical and electronic properties[17,18]. In bioassays, they are mainly used as optical or electrochemical detection labels[19–21]. Their composition with different metals and the size-dependent optical properties even allows the use in multiplexing bioassays. Their utilization as electrochemical detection label in bioassays and biosensors[22] has been mainly carried out by digesting the nanocrystals in acidic media to release the cationic metals to the solution, which are then determined by anodic stripping voltammetry. In early works, the bioassays were typically performed on the surface of microplates as in enzyme-linked immunosorbent assays (ELISA). The acid digestion was also conducted in the microplates, and after releasing the metals, an aliquot of the solution was transferred to a conventional electrochemical cell (with appropriate buffer solution) to perform the voltammetric detection[23,24]. This step is usually performed in presence of a metal such as mercury[25] or bismuth[26], which generates a film able to improve the preconcentration of the metals from the QDs and, therefore, achieve a more sensitive detection. Numerous applications have been described using QDs as detection label of bioassays since it was first introduced in 2002 for the detection of nucleic acid hybridization[23]. QDs have also been used as label in aptasensors showing a good performance in such assays for the detection of small molecules such as thrombin using competitive detection[27]. Likewise, QDs in immunoassays has also shown great results[28]. Although, QDs detection is typically performed with voltammetric techniques, the potentiometric detection in immunoassays has also been described, using H_2O_2 for the digestion of the nanoparticles in order to avoid a drastic change in pH[29]. Many other examples of immunoassays using QDs can be found for detection of proteins[30,24] or even bacteria[31]. However, it is arguable that these systems can be considered biosensors as the recognition element and the transducer are not integrated. In recent years, different methods have been described for the in situ

electrochemical detection of QDs. The strategy is similar to the early works, but both the bioassay as the acid digestion and the electrochemical detection is performed using the same electrode surface, simplifying the overall detection procedure. This strategy has been successfully employed for the detection of biotin in a competitive assay[32], the detection of celiac disease biomarkers, such as anti-transglutaminase IgG and IgA antibodies[33,34], or can even be used to estimate the nanocrystal size[35]. Other published strategies for detecting QDs have been the direct detection of cadmium from the nanoparticle without performing the digestion of the nanoparticle for detecting DNA related to the cystic fibrosis[36], although the detection in this case is much less sensitive as can be seen by the limit of detection of the method[37]. Another interesting approach has been the use of portable flexible devices for performing the detection of QDs within the same microplate wells where the biological reaction is carried out[38]. Recently, we have described the detection of QDs using the stripping signal of silver selectively electrodeposited on the surface of the nanoparticles[39] or by using the stabilizing effect of copper by the nanocrystals[40,41], achieving the direct and sensitive detection of QDs without performing the acid digestion. Although, the utilization of nanoparticles as detection label for biosensors has some advantages to using enzymatic labels, one of its known drawbacks is their lower sensitivity. For this reason, the development of novel methodologies to improve the sensitivity of the electrochemical detection of nanoparticles used as biosensing labels is a constant concern.

In this work, we developed a methodology for the detection of cadmium on screen-printed electrodes using a portable magnetoelectrochemical support, which enhances the mass transfer of the analytes due to forced convection by the MHD effect. This methodology is applied to the detection of QDs at low concentrations, and finally, is applied to the detection of QDs employed as label of electrochemical biosensors using screen-printed electrodes. The neutravidin-biotin affinity reaction and the detection of anti-transglutaminase IgA antibodies (a celiac disease biomarker) using a sandwich-type assay are employed as biosensing models, although the methodology could

work with other biosensing systems.

2. MATERIALS AND METHODS

2.1. Apparatus and electrodes

Electrochemical measurements were performed with a DropSens µStat8000 potentiostat/galvanostat interfaced to an Apple MacBook Air laptop and controlled by DropView 8400 software (version 2.2). All measurements were carried out at room temperature without removing oxygen from the solution. Screen-printed carbon electrodes (SPCEs) were purchased from DropSens. These electrodes incorporate a three-electrode configuration, printed on ceramic substrates (3.4 x 1.0 cm). Both working (disk-shaped 4 mm diameter) and counter electrodes are made of carbon inks, whereas quasireference electrode and electric contacts are made of silver. Unless stated otherwise, a 45 µL drop was placed on the electrode surface to form the electrochemical cell and perform the measurements. All indicated potentials are related to the silver quasireference screen-printed electrode. The SPEs were connected to the potentiostat through a specific connector (DropSens, DRP-CAST). The magnetoelectrochemical support employed throughout this work was developed by DropSens (ref. MAGNETOEC). The support has two neodymium permanent magnets (cylindrical, 20x10 mm) bonded to threaded bolts, allowing them to be positioned at different gaps by moving the bolts. The gap between the magnets establishes the magnetic field applied to the electrode. The magnetoelectrochemical support can be used in vertical and horizontal positions. In this work, the support was used in vertical position and the electrode placed over the inferior magnet as shown in the **Figure 1A**. The gap between the magnets was 3 mm, close enough to create a high magnetic field (0.914 T) and avoiding to touch the drop with the superior magnet. In this configuration, the magnetic field is applied parallel to the gravity force and perpendicular to the electric current. The Lorentz force generated will be maximal (as B and J vectors are perpendicular) and parallel to the electrode surface according to the scheme of the **Figure 1B**, increasing the mass transfer to the screen-printed electrode surface by forced convention due to the MHD effect.

[FIGURE 1]

2.2. Reagents and solutions

The reagents and solutions used in this work are described in the Supporting Information.

2.3. Immunoassay procedures

Immunoassay procedures are described in the Supporting Information. **Figures S1** and **S2** show schematic diagrams of the procedures.

2.4. Voltammetric measurements in biosensors

After the biological reaction, 45 μL of 0.05 M HCl solution with 5 mM Hg(II) and 50 mM Fe(III) were added to release Cd(II) from the QDs nanocrystals. Cadmium was preconcentrated on the electrode surface by applying a potential of -1.1 V for 90 s, simultaneously a mercury film was also formed during this step and Fe(III) ions were reduced to Fe(II). The potential was swept from -1.1 V to -0.8 V using differential pulse voltammetry (DPV) with the following parameters: 10 s as equilibration time, 10 ms as pulse time, 5 mV as potential step, 50 mV as pulse amplitude and 50 mV/s as scan rate. The magnetic field was applied continuously during the deposition and stripping steps.

2.5. Real samples treatment

The determination of biotin in real samples was carried out in multivitamin tablets (Deliplus), bought in a local supplier, with a known concentration of biotin. Each tablet (445 mg) contained 25 μg of biotin. One tablet was dissolved in 100 mL of Tris buffer and a 1:20 dilution was performed in order to get a solution with a biotin concentration within the dynamic range of the calibration plot. An aliquot of 30 μL of this solution, which also contained 1.5 nM of BT-QDs, was placed on the biosensor modified with neutravidin to conduct the competitive assay as explained previously.

The determination of anti-tTG IgA antibodies in samples was carried out by spiking human serum with different concentrations of anti-tTG IgA antibodies (5, 15 and 30 U/mL) using the calibrators

of the commercial ELISA kit. A dilution 1:2 was performed with Tris buffer and 30 µL of this solution was placed on the immunosensor modified with tTG to conduct the sandwich assay as described in the previous section.

3. RESULTS AND DISCUSSION

3.1. Magnetoelectrochemical detection of cadmium-based quantum dots

The aim of this section was to evaluate the ability of the magnetoelectrochemical support to increase the mass transfer in the electrochemical deposition of cadmium released from CdSe/ZnS QDs using screen-printed electrodes. After the deposition, the stripping of cadmium is performed using a suitable voltammetric technique, obtaining a stripping peak whose magnitude is proportional to the initial amount of cadmium. The applied magnetic field was always at 0.917 T by placing the magnets at a distance of 3 mm. Therefore, the increased mass transfer and the enhanced deposition efficiency by the MHD effect must occur by increasing the current during the cadmium deposition, as indicated by **equation 1**. However, the current increment cannot be solely produced by the reduction of cadmium as the aim of the method is the detection of very small concentrations of Cd(II), whose reduction will produce a small current and the Lorentz force generated will also be small. Therefore, the use of a chemical species at higher concentrations than cadmium, which can be reduced simultaneously at the cadmium reduction potential is mandatory. This species must not adversely influence the deposition/stripping of cadmium by competing for the same active surface sites, have a close oxidation potential or even by causing a negative effect in the capacitive current preventing the visualization of the cadmium stripping process. Several species have been described as pumping species such as Fe(III), BQ or even the Hg(II) employed for the formation of a metallic film to improve the preconcentration[9,11,10]. Other species such as $[Fe(CN_6)]^{3-}$ or $[Ru(NH_3)_6]^{3+}$ could also be valid because their reduction occurs at potentials more positive than the reduction of cadmium. In our case, after initial evaluation of these species, Fe(III) was employed for subsequent

studies as it did not produce a negative influence on the cadmium signal and it has a lower toxicity compared to other of the mentioned species. **Figure 2A** shows the voltammetric response obtained for a solution of 100 µg/L of Cd(II) in the presence and absence of 20 mM Fe(III) and in the presence and absence of 0.5 mM Hg(II) in HCl 0.01 M. HCl was used as electrolyte because it is useful for releasing Cd(II) ions from the QDs as has been previously described[32,35]. The presence of Hg(II) in solution for the *in-situ* generation of a mercury film improves significantly the signal obtained for Cd(II) due to the improvement of the preconcentration as has been widely described in the literature[42]. Furthermore, the presence of 20 mM Fe(III) in solution does not affect the magnitude of the stripping peak current but the peak potential. Moreover, the deposition of iron does not occur at the potentials employed for the cadmium electrodeposition (as can be observed in the voltammogram obtained in absence of Cd(II)). The peak potential shifted towards more negative potentials suggesting that the oxidation of cadmium deposited on the electrode surface occurs more easily. This fact might be explained by the increased ion flow caused by the reduction of Fe(III) that produces a convective effect on the electrode surface favouring the oxidation of cadmium during the stripping voltammetry sweep as Fe(III) continues to be reduced at these potentials. **Figure 2B** shows the voltammograms in presence and absence of the magnetic field applied by the magnetoelectrochemical support. In the absence of Fe(III), the voltammograms obtained are similar to those obtained in absence of the magnetic field, indicating that under these conditions the magnetic field is unable to generate sufficient hydrodynamic flow to enhance the cadmium preconcentration. However, when 20 mM of Fe(III) are added to the solution, a significant increment in the stripping peak current is observed, suggesting the enhancement in the preconcentration step due to the increased hydrodynamic flow created by the magnetic field to the solution droplet, and therefore, Fe(III) presence is essential to produce the enhancing effect. Reduction currents generated in the different conditions were evaluated by chronoamperometry as discussed in the Supporting Information (**Figure S3**). A new shift in the peak potential towards more negative values is observed in the voltammograms with Fe(III) and the magnetic field,

indicating a similar effect to the mentioned previously. Therefore, it seems that the shift of the peak potential could be due to the convective effect produced on the electrode surface, which promotes cadmium stripping. Numerical simulations have shown that when a potential step is applied (as in voltammetry) a vortex is generated near the electrode surface[43] with a flow direction that could help the removal of the metal from the electrode surface. This fact was confirmed by removing the magnetoelectrochemical support just before the stripping step (**Figure S4**). In these conditions the potential of the stripping peak was similar with and without the magnetic field applied. Although other authors have reported that the magnetic field applied in the stripping step enhances the peak current (at extremely low scan rates)[13], in our case the shift on the peak potential did not influence the stripping peak current significantly, and for that reason, the magnetoelectrochemical support was not removed during the stripping step. As shown in **Figure 2B**, even under initial conditions, an improvement of the analytical signal was achieved in the presence of the magnetic field applied by the magnetoelectrochemical support to screen-printed electrodes.

[FIGURE 2]

Then, the experimental conditions were optimized in order to enhance the detection of Cd(II), which is the species released by the CdSe/ZnS QDs employed as electrochemical label for biosensors as discussed later. The effect of several parameters on the stripping peak current of Cd(II) was evaluated in presence of the magnetic field. The influence of HCl concentration used as electrolyte medium was evaluated (**Figure S5**). HCl concentration was tested between 0.005 and 0.1 M but a moderate effect on the analytical signal was found in the absence and presence of the magnetic field. However, slightly better conditions were found at a concentration of 0.05 M of HCl, so this concentration was employed in the subsequent studies. The utilization of a high HCl concentration as electrolyte medium could allow to avoid the acid digestion step of the QDs. QDs should have a low stability in an acidic medium such as 0.05 M HCl and the nanoparticle should be

digested releasing the metals to the solution. The effect of the Hg(II) concentration employed to generate the Hg film on the electrode surface was also evaluated (**Figure S6**). The results show an increment in the cadmium stripping peak current in the presence and absence of the magnetic field with increasing concentrations of Hg(II) in solution up to 25 mM. Although, the use of micro-droplets with screen-printed electrodes is a clear advantage in order to minimize the amount of waste generated, a concentration of 5 mM Hg(II) was chosen due to the potential toxicity of mercury. Under these conditions, the signal increased by about 145% after the application of the magnetic field compared to the signal in absence of the magnetic field. The concentration of Fe(III) species, used for the increment of the hydrodynamic flow, also plays an important role to enhance the analytical signal in the presence of the magnetic field. Several concentrations of Fe(III) were evaluated (**Figure S7A**), obtaining a practically constant value for the stripping peak current in the absence of the magnetic field, but an increment was clearly observed in the presence of the magnetic field up to 50 mM Fe(III). The enhancement of the peak current under these conditions was 192% compared to the signal in absence of the magnetic field. These results show that high concentrations of Fe(III) did not influence the electrochemical detection of Cd(II) because they do not compete for the active sites in the Hg film and the Fe(II) species generated is soluble in acidic media avoiding to decrease the electrode area. For concentrations above 100 mM of Fe(III), a decrease in the signal was observed in the presence of the magnetic field because the peak potential is shifted to a potential rather negative (close to the initial potential), and the preconcentration in these cases was lower. The evaluation of these Fe(III) concentrations using a more negative deposition potential (-1.2 V) showed similar results (**Figure S7B**), so 50 mM of Fe(III) was chosen as the most suitable concentration for enhancing the cadmium detection using the magnetoelectrochemical support. **Figure S8** shows the voltammograms obtained for several concentrations of Fe(III) in presence and absence of the magnetic field. The shift of the peak potentials depends strongly on the Fe(III) concentration. Moreover, the peak potential shift occurred

to a greater extent in the presence of the magnetic field. Therefore, it seems clear that the convective effect favouring the oxidation of cadmium is due mainly to the reduction of Fe(III).

The effect of the deposition potential and time was evaluated. In this case, both parameters could affect both signals in presence and absence of the magnetic field. **Figure S9** shows the effect of both parameters in the stripping peak currents. A low range of deposition potentials were evaluated (from -1.1 V to 1.3 V) because the peak potential in the presence of the magnetic field is close to -1.1 V, while that more negative potentials than -1.3 V increased significantly the capacitive current and the stripping peak was affected, specially for measurements in the absence of the magnetic field. No significant changes in the stripping peak currents were observed for the deposition potentials evaluated. Therefore, a potential of -1.1 V was selected because the stripping peak was perfectly detected with a flat baseline and lower capacitive currents. The deposition time increased the peak currents in both the presence and absence of the magnetic field. The enhancement of the peak current remained close to 200% for all cases. 90 s as deposition time was chosen because it increased the peak currents compared to lower times and the analysis time is relatively short. However, if analysis with lower detection limits were necessary, the increment of the deposition time could improve the cadmium preconcentration at the expense of increasing the time of analysis. It is interesting to show that the deposition time does not influence the blank signal, which remains close to zero, indicating a small presence of impurities in the solution even using a high concentration of the Fe(III) salt.

The total charge under the voltammetric peak (Q_{ads}) can be used to estimate values of the cadmium surface coverage (Γ_{ads}) deposited on the screen-printed electrode surface according to the following equation:

$$Q_{ads} = nFA\Gamma_{ads} \quad \textbf{(X)}$$

where n is the number of exchanged electrons, F is the Faraday constant and A is the electrode area. It seems clear that the preconcentration in the presence of the magnetic field is greater than in the absence due to the improved mass transfer to the electrode surface. The effect of the magnetic field in the preconcentration capacity was evaluated for different concentrations of Cd(II): 25, 50 and 100 μg/L. **Figure S10** shows the voltammograms obtained for these concentrations under the experimental conditions optimized in presence and absence of the magnetic field. The values obtained for the surface coverage are shown in the **Table S1**. These values were between 0.1 and 1 nmol/cm^2. It appears that the concentration of Cd(II) in solution does not significantly influence the preconcentration capacity. It is also interesting to mention that in absence of the magnetic field, the preconcentration step is only capable of depositing about 15-18% of the initial cadmium in solution, while if the preconcentration step is performed applying the magnetic field, the yield increases up to 37% of the initial cadmium in solution. Although this yield is far from 100 %, the enhancement is significant. Furthermore, as explained previously, if the deposition time were increased, this yield could also be higher.

The optimized method was applied to the detection of QDs. 2 μL of a QDs solution (diluted in ultrapure water) was placed on the working electrode surface and 45 μL of the measurement solution (5 mM Hg(II), 20 mM Fe(III), 0.05 M HCl) was dropped over the QDs solution. **Figure S11** shows the voltammetric response obtained in the presence and absence of the magnetic field using a QDs solution at a concentration of 1 nM. The utilization of HCl 0.05 M as electrolytic medium was enough to get the acid digestion of the nanoparticles to release Cd(II) to the solution suggested by the high stripping peak currents obtained. An enhanced signal is obtained in presence of the magnetic field, proving that the magnetoelectrochemical support is capable of increasing the voltammetric signal of QDs. A calibration curve was registered with increasing concentrations of QDs in order to compare the analytical performance with other electrochemical detection methods of QDs. **Figure 3** shows the voltammograms obtained for the different concentrations of QDs (in

presence of the magnetic field) and the associated calibration plot (in presence and absence of the magnetic field). A linear range between 0.05 and 5 nM was found in presence of the magnetic field and between 0.1 and 5 nM in absence of the magnetic field. In absence of the magnetic field, the linear relationship between the peak current and the QDs concentration followed the equation: i_p (μA) = 0.01 (±0.06) + 7.42 (±0.08) [QDs](nM), R^2 = 0.994, n=3, RSD (slopes) = 5.0%. In presence of the magnetic field, the linear relationship between the peak current and the QDs concentration followed the equation: i_p (μA) = 0.01 (±0.08) + 15.5 (±0.1) [QDs](nM), R^2 = 0.995, n=3, RSD (slopes) = 8.8%. The limits of detection (calculated as the concentration corresponding to three times the standard deviation of the estimate[44]) were 0.1 and 0.05 nM, respectively. Considering the sample volume (2 μL), the detection limit in presence of the magnetoelectrochemical support corresponds to just $6x10^7$ nanoparticles (100 amol of QDs). The magnetoelectrochemical support improved the analytical performance of the QDs detection and the method developed improved the electrochemical detection methods previously published in the literature, listed in **Table S2**. Therefore, it is expected that this method is particularly interesting for the detection of electrochemical biosensors using QDs as label.

[FIGURE 3]

3.2. Magnetoelectrochemical detection of quantum dots for biosensing applications

The method was applied to the detection of QDs used as label for electrochemical biosensors. Firstly, the behaviour was checked in a simple system such as the biotin-neutravidin affinity reaction and then applied in an immunosensor system for the detection of anti-transglutaminase IgA antibodies. The methodology was similar in both cases: modification of the screen-printed working electrode surface with the recognition element and conducting the bioassay in several steps. QDs detection is carried out using the optimized method described in the previous section. It should be noted that the use of media able to digest the QDs used as labels to release Cd(II) to the solution is essential because if the label remains fixed on the electrode surface (and the detection is direct), the

magnetohydrodynamic effect would not be able to improve the mass transfer, and therefore, no increment in the sensitivity would be observed.

3.2.1. Biotin detection

The system employed for the detection of biotin was similar to one previously reported in our group[32] with some variations. The modification of the electrode surface was carried out with neutravidin since it is a protein with lower cost than streptavidin and they present similar affinity characteristics. Then, the electrode surface was blocked by a solution of 2% BSA, in order to avoid the non-specific adsorption, and a solution of BT-QDs was added for the affinity reaction with neutravidin on the electrode surface (**Figure S1**). Increasing concentrations of BT-QDs were evaluated to obtain a calibration plot in terms of concentration of QDs. **Figure S12** shows the voltammograms obtained and the associated calibration plots in presence and absence of the magnetic field (applied only in the electrochemical detection step). The linear range in presence of the magnetic field was between 0.01 and 1.5 nM of BT-QDs and in absence of the magnetic field was between 0.025 and 1.5 nM of BT-QDs. In absence of the magnetic field, the linear relationship between the peak current and the BT-QDs concentration followed the equation: i_p (μA) = 0.4 (±0.1) + 40.2 (±0.7) [BT-QDs](nM), R^2 = 0.998, n=3, RSD (slopes) = 5.6%. In presence of the magnetic field, the linear relationship between the peak current and the QDs concentration followed the equation: i_p (μA) = 0.53 (±0.09) + 62 (±1) [QDs](nM), R^2 = 0.998, n=3, RSD (slopes) = 8.2%. The limits of detection (calculated as the concentration corresponding to three times the standard deviation of the estimate) were 0.004 and 0.008 nM, respectively. The magnetoelectrochemical support improves the sensitivity and limit of detection of QDs used as electrochemical label. In this case, the improvement of the sensitivity was about 155%, lower than in the previous studies. This fact is probably due to the great amount of proteins present in the electrode surface after the biological assay or released to the solution after dropping the acidic medium. The local viscosity of the solution could be higher and the effect of the hydrodynamic force created by the magnetic field

could be lower[45,46]. It also influences the shift of the peak potential, lowering the gap between the peak potentials when the magnetic field is applied and without magnetic field. In any case, the increased sensitivity could be very interesting in competitive assays where small concentrations of analyte may lead to high signal changes when the magnetoelectrochemical support is used. Compared to the previous work developed in our group[32], the new method lowered the limit of detection in almost two orders of magnitude (from 0.2 to 0.004 nM) and an approximate improvement of 2000% on the sensitivity of the response (from 23.9 to 489.7 $\mu A\ nM^{-1}\ cm^{-2}$) was also achieved.

In order to perform the determination of biotin in real samples, a calibration curve was registered following a competitive bioassay. In this approach, the free BT and BT-QDs compete for the binding sites of NTV on the electrode surface. A scheme of this methodology was shown in the **Figure S1**. Free BT can bind to neutravidin avoiding the reaction between BT-QDs and NTV, and after washing, a decreasing response is obtained with increasing concentrations of free biotin, obtaining the maximum signal in absence of biotin. Considering the BT-QDs calibration plot described in the previous paragraph, a concentration of 1.5 nM of BT-QDs was chosen as the most suitable in order to detect small concentrations of free BT. **Figure 4** shows the voltammograms obtained and the associated calibration plot (semilogarithmic response) in presence of the magnetic field. A linear dependence between i/i_0 (%) and the logarithm of the concentration of free biotin was obtained from $1x10^{-10}$ to $5x10^{-7}$ M, where i_0 is the current obtained in the absence of biotin, and i is the current obtained when free biotin is present in solution. The dynamic range was estimated between $1.6x10^{-10}$ and $8.45x10^{-8}$ M (response between 20 and 80% of the maximum signal), following a method described in the literature for a semilogarithmic response[47,48]. The limit of detection estimated was $0.6x10^{-10}$ M (signal obtained for a decrement of 10% from the maximum response). The reproducibility between the slopes of the calibration curves (n=3) was of 8.2% (in terms of RSD). A comparison with some electrochemical methods for the determination of biotin

proposed in the literature (**Table S3**) shows that our sensor is quite competitive in terms of detection limits and linear range against other biosensors (or bioassays) where enzymatic detection labels or amplified labels such as liposomes are used. Just one case, in which the detection is performed in a flow injection analysis system and with magnetic preconcentration, presents better analytical characteristics than our sensor. This demonstrates the good performance of QDs as electrochemical label and the magnetoelectrochemical support as a system to improve biosensing applications. Moreover, our system also allows the *in situ* detection of QDs in the same platform where the bioassay is performed. Using the calibration plot obtained, the determination of biotin in multivitamin tablets was carried out. **Table S4** shows the results obtained experimentally, showing a good agreement between the results obtained with the method developed in this work and the amount according to the specifications of the multivitamin tablets.

[FIGURE 4]

3.2.2. Detection of anti-tissue transglutaminase IgA antibodies

The detection of anti-tTG IgA antibodies was performed following the immunological sandwich-type assay on the screen-printed electrode surface previously described. The electrode surface was modified with tTG, which acts as the recognition element. Non-specific adsorptions were avoided by blocking with BSA as reported in previous works[49]. The sensor is incubated with serum solutions from a commercial ELISA kit with known concentrations (calibrators) or positive and negative controls. The sandwich immunodetection is performed by incubating the sensor with anti-IgA-BT antibodies and QDs-STV (in subsequent steps) as shown in **Figure S2**. The concentrations and conditions employed were similar to those employed in our previous work[34]. QDs detection was carried out with the experimental conditions optimized in the previous sections and using the magnetoelectrochemical support (also without the magnetoelectrochemical support for comparison). **Figure S13** shows the voltammograms obtained using the biosensor for the positive and negative control sera in presence and absence of the magnetic field. As expected, the peak current increases significantly in presence of the magnetic field, proving that the

magnetoelectrochemical support also works in complex biosensing systems such as this sandwich assay. A calibration curve was registered with increasing concentrations of anti-tTG IgA antibodies from the serum calibrators of the commercial ELISA kit. **Figure 5** shows the voltammograms obtained in presence of the magnetic field and the associated calibration plots (in presence and absence of the magnetic field). The linear range for both cases was between 3 and 40 U/mL of anti-tTG IgA antibodies. In absence of the magnetic field, the linear relationship between the peak current and the anti-tTG IgA concentration followed the equation: i_p (μA) = 0.5 (±0.1) + 0.40 (±0.01) [anti-tTG IgA](U/mL), R^2 = 0.990, n=3, RSD (slopes) = 4.6%. In presence of the magnetic field, the linear relationship between the peak current and the QDs concentration followed the equation: i_p (μA) = 0.8 (±0.2) + 0.74 (±0.01) [anti-tTG IgA](U/mL), R^2 = 0.996, n=3, RSD (slopes) = 7.0%. The limits of detection (calculated as the concentration corresponding to three times the standard deviation of the estimate) were 1.7 and 1.0 U/mL, respectively. According to the specifications of the commercial ELISA kit, the cut-off values to evaluate the results are the following ones: negative if the concentration is less than 5 U/mL, indeterminate between 5 and 8 U/mL and positive if the concentration is above 8 U/mL. Therefore, the immunosensor developed with the aid of the magnetoelectrochemical support is able to differentiate easily these key concentrations. It is interesting to compare the analytical characteristics obtained for this immunosensor with those of other biosensors published previously in the literature for the determination of anti-tTG IgA antibodies. Our group has previously developed a similar immunosensor but using alkaline phosphatase (an enzyme) as label[50,49]. This immunosensor had a sensitivity of 4.2 μA U^{-1} mL cm^{-2} that was superior to the sensitivity of another immunosensor also developed by our group[34] using Cd-based QDs as label and the detection of Cd by a bismuth film (2.9 μA U^{-1} mL cm^{-2}). However, the sensitivity obtained by the immunosensor described in this work (5.9 μA U^{-1} mL cm^{-2}) is significantly higher than those of the mentioned immunosensors. This fact is due to the magnetoelectrochemical support, which improves significantly this analytical parameter. Other analytical characteristics such as linear range or precision are similar to those

obtained by the sensor developed in this work, but the estimated limit of detection (1.0 U/mL) is lower due to the higher sensitivity and the low non-specific adsorption. There are other works that describe the development of immunosensors for the detection of anti-tTG IgA antibodies[51–55], but its analytical comparison is complicated due to using different concentrations units.

[FIGURE 5]

Finally, the immunosensor was evaluated with real samples. Human serum was spiked with three different concentrations of anti-tTG IgA antibodies (5, 15 and 30 U/mL) using the calibrators of the commercial ELISA kit and were determined using the biosensor in presence of the magnetic field. Furthermore, the concentration of anti-tTG IgA in the positive and negative controls of the kit were also estimated. **Table S4** shows the results obtained, which are in good agreement with the expected results (spiked concentrations and concentrations indicated in the specifications of the commercial ELISA kit). The magnetoelectrochemical support employed in this work allows the determination of low concentrations of anti-tTG IgA in real samples as human serum.

4. CONCLUSIONS

A portable magnetoelectrochemical support (with two permanent magnets) is able to enhance the mass transfer of ions in a quiescent solution droplet, which compose the electrochemical cell of screen-printed electrodes. A forced convection (produced by the Lorentz force) is generated in the droplet under the magnetic field. This effect was used to improve the efficiency of the electrodeposition of cadmium released from quantum dots, employed as detection label of biosensors. Thus, the magnetoelectrochemical support improves the electrochemical detection of such nanoparticles (in terms of limits of detection and sensitivity). On one hand, the method developed and optimized is applied successfully to the detection of biotin in a vitamin supplement by a competitive assay, and, on the other hand, it is also applied to the detection of a celiac disease biomarker in human serum samples. The analytical characteristics estimated for both biosensors

improve those obtained for similar biosensors using nanostructured labels previously described in the literature, even approaching to the sensitivity of biosensors that use enzymatic labels, typically more sensitive. Therefore, we described in this work how magnetoelectrochemistry can be used to enhance the detection in portable and disposable electrochemical biosensors and in similar applications.

ACKNOWLEDGEMENTS

This work has been supported by the FC-15-GRUPIN-021 project from the Asturias Regional Government and the CTQ2014-58826-R project from the Spanish Ministry of Economy and Competitiveness (MEC). Daniel Martín-Yerga thanks the MEC for the award of a FPI grant (BES-2012-054408).

REFERENCES

1. A. Alemany and J. P. Chopart, *Fluid Mech. its Appl.*, 2007, **80**, 391–407.
2. L. M. A. Monzon and J. M. D. Coey, *Electrochem. commun.*, 2014, **42**, 42–45.
3. K. Ngamchuea, K. Tschulik, and R. G. Compton, *Nano Res.*, 2015, **8**, 3293–3306.
4. L. M. A. Monzon and J. M. D. Coey, *Electrochem. commun.*, 2014, **42**, 38–41.
5. S. R. Ragsdale, K. M. Grant, and H. S. White, *J. Am. Chem. Soc.*, 1998, **120**, 13461–13468.
6. I. Mogi and M. Kamiko, *J. Cryst. Growth*, 1996, **166**, 276–280.
7. H. Matsushima, T. Nohira, I. Mogi, and Y. Ito, *Surf. Coatings Technol.*, 2004, **179**, 245–251.
8. O. Devos, O. Aaboubi, J.-P. Chopart, A. Olivier, C. Gabrielli, and B. Tribollet, *J. Phys. Chem. A*, 2000, **104**, 1544–1548.
9. E. A. Clark and I. Fritsch, *Anal. Chem.*, 2004, **76**, 2415–2418.
10. A. A. Ensafi, Z. Nazari, and I. Fritsch, *Analyst*, 2012, **137**, 424–431.
11. E. C. Anderson and I. Fritsch, *Anal. Chem.*, 2006, **78**, 3745–3751.
12. M. C. Weston, E. C. Anderson, P. U. Arumugam, P. Y. Narasimhan, and I. Fritsch, *Analyst*, 2006, **131**, 1322–1331.
13. Y. M. Panta, S. Qian, and M. A. Cheney, *J. Colloid Interface Sci.*, 2008, **317**, 175–182.
14. Y. P. Gao, W. Z. Wei, X. H. Gao, J. X. Zeng, and J. Yin, *Int. J. Environ. Anal. Chem.*, 2007, **87**, 521–533.
15. M. C. Weston, C. K. Nash, and I. Fritsch, *Anal. Chem.*, 2010, **82**, 7068–7072.
16. M. C. Weston, C. K. Nash, J. J. Homesley, and I. Fritsch, *Anal. Chem.*, 2012, **84**, 9402–9409.
17. A. P. Alivisatos, *Science (80-.).*, 1996, **271**, 933–937.
18. M. Amelia, C. Lincheneau, S. Silvi, and A. Credi, *Chem. Soc. Rev.*, 2012, **41**, 5728–5743.
19. J. M. Costa-Fernández, R. Pereiro, and A. Sanz-Medel, *TrAC, Trends Anal. Chem.*, 2006, **25**, 207–218.
20. F. Lisdat, D. Schäfer, and A. Kapp, *Anal. Bioanal. Chem.*, 2013, **405**, 3739–3752.
21. R. Gill, M. Zayats, and I. Willner, *Angew. Chemie Int. Ed.*, 2008, **47**, 7602–7625.

22. C. Kokkinos and A. Economou, *Anal. Chim. Acta*, 2017, **961**, 12–32.

23. J. Wang, G. Liu, and A. Merkoçi, *J. Am. Chem. Soc.*, 2003, **125**, 3214–3215.

24. J. Wang, G. Liu, H. Wu, and Y. Lin, *Small*, 2008, **4**, 82–86.

25. D. Tang, L. Hou, R. Niessner, M. Xu, Z. Gao, and D. Knopp, *Biosens. Bioelectron.*, 2013, **46**, 37–43.

26. D. Du, J. Ding, Y. Tao, H. Li, and X. Chen, *Biosens. Bioelectron.*, 2008, **24**, 869–874.

27. J. A. Hansen, J. Wang, A.-N. Kawde, Y. Xiang, K. V Gothelf, and G. Collins, *J. Am. Chem. Soc.*, 2006, **128**, 2228–2229.

28. G. Liu, J. Wang, J. Kim, M. R. Jan, and G. E. Collins, *Anal. Chem.*, 2004, **76**, 7126–7130.

29. R. Thürer, T. Vigassy, M. Hirayama, J. Wang, E. Bakker, and E. Pretsch, *Anal. Chem.*, 2007, **79**, 5107–5110.

30. H. Wu, G. Liu, J. Wang, and Y. Lin, *Electrochem. Commun.*, 2007, **9**, 1573–1577.

31. M. Freitas, S. Viswanathan, H. P. A. Nouws, M. B. P. P. Oliveira, and C. Delerue-Matos, *Biosens. Bioelectron.*, 2014, **51**, 195–200.

32. D. Martín-Yerga, M. B. González-García, and A. Costa-García, *Sens. Actuators B*, 2013, **182**, 184–189.

33. D. Martín-Yerga, M. B. González-García, and A. Costa-García, *Talanta*, 2014, **130**, 598–602.

34. D. Martín-Yerga and A. Costa-García, *Bioelectrochemistry*, 2015, **105**, 88–94.

35. D. Martín-Yerga, D. Bouzas-Ramos, M. Menéndez-Miranda, A. R. M. Bustos, J. R. Encinar, J. M. Costa-Fernández, A. Sanz-Medel, and A. Costa-García, *Electrochim. Acta*, 2015, **166**, 100–106.

36. S. Marín and A. Merkoçi, *Nanotechnology*, 2009, **20**, 55101.

37. A. Merkoçi, L. H. Marcolino-Junior, S. Marín, O. Fatibello-Filho, and S. Alegret, *Nanotechnology*, 2007, **18**, 35502.

38. C. Kokkinos, A. Economou, T. Speliotis, P. Petrou, and S. Kakabakos, *Anal. Chem.*, 2015, **87**, 853–857.

39. D. Martín-Yerga, E. C. Rama, and A. Costa-García, *Anal. Chem.*, 2016, **88**, 3739–3746.

40. D. Martín-Yerga and A. Costa-García, *Electrochem. Commun.*, 2017, **74**, 53–56.

41. D. Martín-Yerga and A. Costa-García, *Phys. Chem. Chem. Phys.*, 2017, **19**, 5018–5027.

42. A. Economou and P. R. Fielden, *Analyst*, 2003, **128**, 205–212.

43. D. Sen, K. M. Isaac, N. Leventis, and I. Fritsch, *Int. J. Heat Mass Transf.*, 2011, **54**, 5368–5378.

44. J. N. Miller and J. C. Miller, *Statistics and Chemometrics for Analytical Chemistry*, Pearson Education Limited, Essex, England, 2010.

45. N. Leventis, M. Chen, X. Gao, M. Canalas, and P. Zhang, *J. Phys. Chem. B*, 1998, **102**, 3512–3522.

46. O. Lioubashevski, E. Katz, and I. Willner, *J. Phys. Chem. C*, 2007, **111**, 6024–6032.

47. Y. Sugawara, S. J. Gee, J. R. Sanborn, S. D. Gilman, and B. D. Hammock, *Anal. Chem.*, 1998, **70**, 1092–1099.

48. C. Wei, S. Ding, H. You, Y. Zhang, Y. Wang, X. Yang, and J. Yuan, *PLoS One*, 2011, **6**, e29196.

49. M. M. P. S. Neves, M. B. González-García, H. P. A. Nouws, and A. Costa-García, *Biosens. Bioelectron.*, 2012, **31**, 95–100.

50. M. M. P. S. Neves, M. B. González-García, C. Delerue-Matos, and A. Costa-García, *Sens. Actuators B*, 2013, **187**, 33–39.

51. T. Balkenhohl and F. Lisdat, *Analyst*, 2007, **132**, 314–322.

52. M. I. Pividori, A. Lermo, A. Bonanni, S. Alegret, and M. del Valle, *Anal. Biochem.*, 2009, **388**, 229–234.

53. S. Dulay, P. Lozano-Sánchez, E. Iwuoha, I. Katakis, and C. K. O'Sullivan, *Biosens. Bioelectron.*, 2011, **26**, 3852–3856.

54. G. Adornetto, G. Volpe, A. De Stefano, S. Martini, G. Gallucci, A. Manzoni, S. Bernardini, M. Mascini, and D. Moscone, *Anal. Bioanal. Chem.*, 2012, **403**, 1191–1194.

55. S. V Kergaravat, L. Beltramino, N. Garnero, L. Trotta, M. Wagener, M. Isabel Pividori, and S. R. Hernandez, *Biosens. Bioelectron.*, 2013, **48**, 203–209.

TABLES AND FIGURES

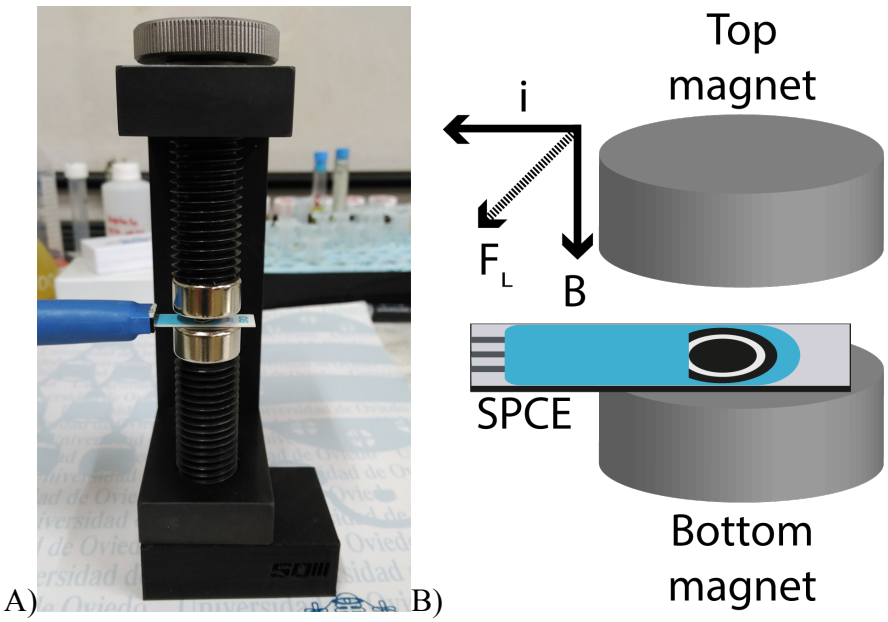

Figure 1. **A)** Picture of the magnetoelectrochemical support positioned vertically with a screen-printed electrode placed between the two permanent magnets. **B)** Scheme of the direction of the magnetic field, current density and the Lorentz force generated by their interaction.

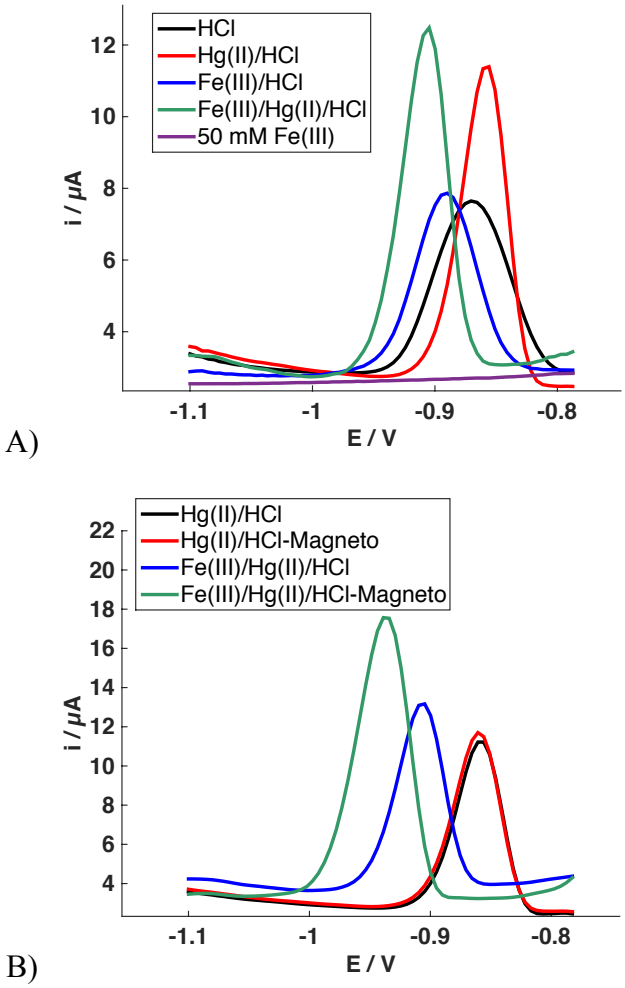

Figure 2. A) Differential-pulse voltammograms of a solution containing 100 µg/L of Cd(II) in absence of Hg(II) and Fe(III) (black), in presence of 0.5 mM Hg(II) (red line), in presence of 20 mM Fe(III) (blue line), in presence of 0.5 mM Hg(II) and 20 mM Fe(III) (green line). The voltammogram of 50 mM Fe(III) in absence of Cd(II) is also presented for comparison (purple line). **B)** Differential-pulse voltammograms of a solution of 100 µg/L of Cd(II) in absence of the magnetic field with 0.5 mM Hg(II) (black line), with 20 mM Fe(III) and 0.5 mM Hg(II) (blue line) and in presence of the magnetic field with 0.5 mM Hg(II) (red line) and with 0.5 mM Hg(II) and 20 mM Fe(III) (green line). Anodic stripping voltammetry was used in both cases by applying a deposition potential of -1.1 V for 45 s.

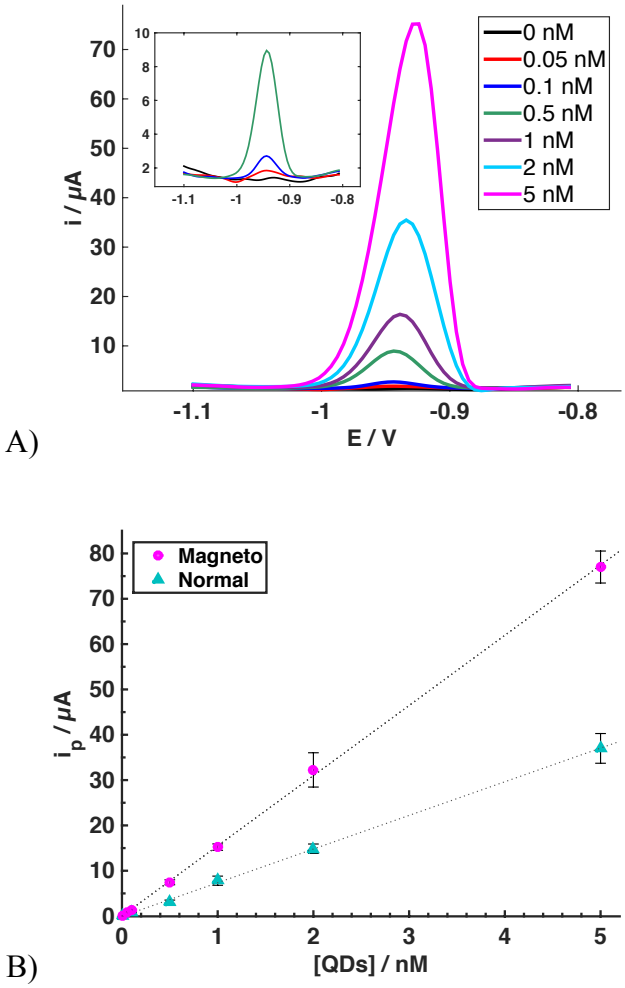

Figure 3. A) Differential-pulse voltammograms of solutions containing 45 µL of 5 mM Hg(II), 50 mM Fe(III), 0.05 M HCl and 2 µL of QDs (in H_2O) at different particle concentrations (0, 0.05, 0.1, 0.5, 1, 2 and 5 nM) in presence of the magnetic field. Inset shows the DPV responses for the lowest concentrations of QDs. **B)** Associated calibration plots in presence and absence of the magnetic field.

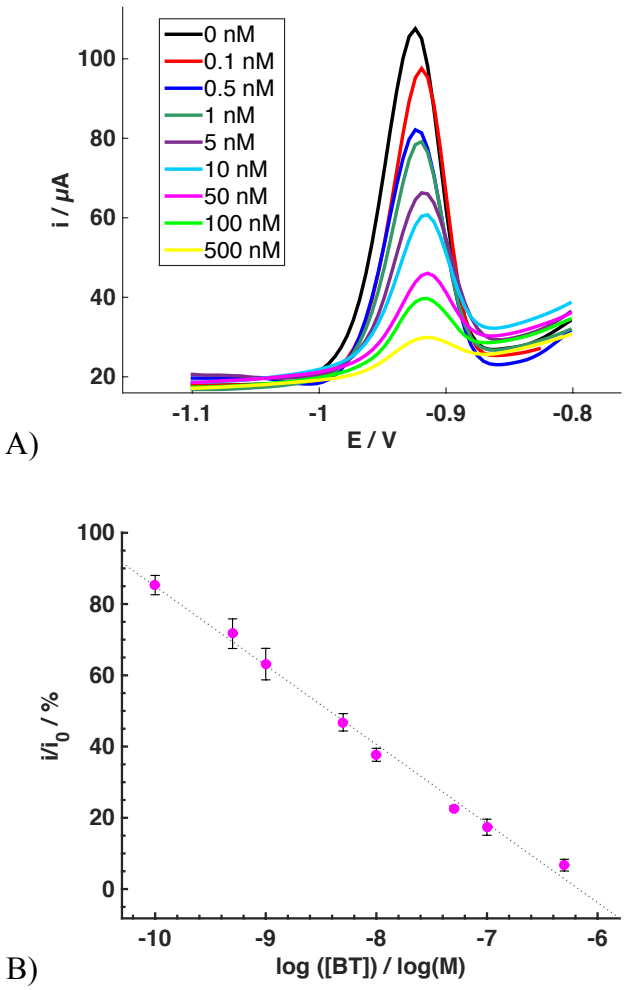

Figure 4. A) Differential-pulse voltammograms for the competitive biosensor for the detection of BT at different concentrations (0, 0.1, 0.5, 1, 5, 10, 50, 100 and 500 nM) in presence of the magnetic field. Procedure of the biosensor is described in section 2.3. **B)** Associated semilogarithmic plot of the calibration curve.

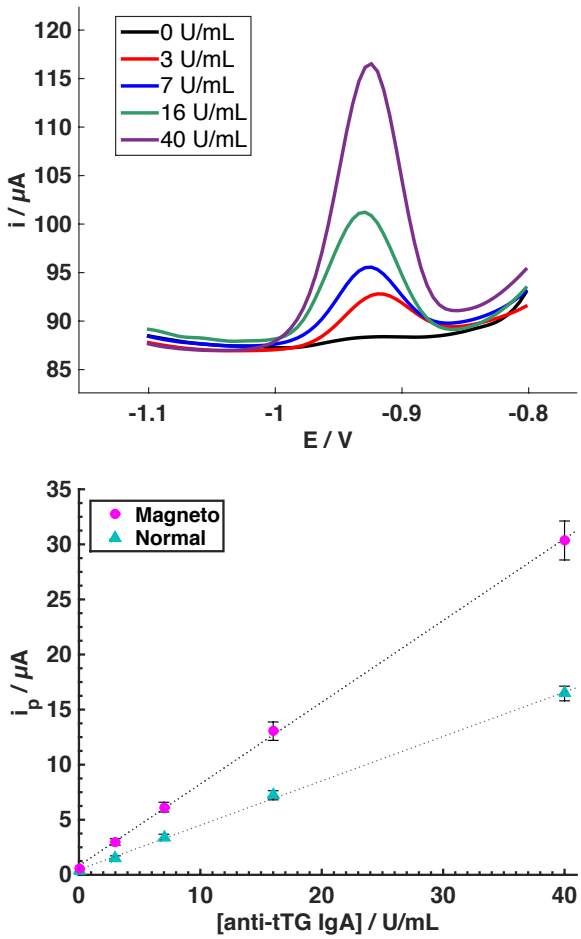

Figure 5. A) Differential-pulse voltammograms for the biosensor performed for the detection of anti-tTG IgA antibodies using calibrators of different concentrations (0, 3, 7, 16 and 40 U/mL) in presence of the magnetic field. Procedure of the biosensor is described in section 2.3. **B)** Associated calibration plots in presence and absence of the magnetic field.

SUPPORTING INFORMATION

Enhanced detection of quantum dots by the magnetohydrodynamic effect for electrochemical biosensing

Daniel Martín-Yerga[1], Pablo Fanjul-Bolado[2], David Hernández-Santos[2], and Agustín Costa-García[1*]*

[1] Departamento de Química Física y Analítica, Universidad de Oviedo, 33006 Oviedo, Asturias, Spain.

[2] DropSens, S.L., Edificio CEEI, Parque Tecnológico de Asturias, 33428 Llanera, Asturias, Spain

*E-mails: martindaniel@uniovi.es; costa@uniovi.es

REAGENTS AND SOLUTIONS

Cadmium(II) standard, mercury(II) acetate, iron(III) nitrate, d-biotin, Tris(hydroxymethyl)aminomethane (Tris), bovine serum albumin fraction V (BSA) and human serum (from human male AB plasma) were purchased from Sigma-Aldrich. Fuming hydrochloric acid (37%) was purchased from Merck. Human tissue transglutaminase (recombinantly produced in insect cells) was purchased from Zedira. Qdot® 655 streptavidin conjugate (QD-STV), biotinylated goat anti-human IgA (anti-H-IgA-BT), Qdot® 655 biotin conjugate (BT-QDs) were purchased from Life Technologies. Neutravidin was purchased from ThermoFisher Scientific. Varelisa Celikey tissue transglutaminase IgA ELISA kit was purchased from Phadia. Each kit contained six human serum calibrators (0, 3, 7, 16, 40, 100 U mL^{-1}) and a positive and a negative control. Ultrapure water obtained with a Millipore Direct Q5™ purification system from Millipore Ibérica S.A. was used throughout this work. All other reagents were of analytical grade. Working solutions of neutravidin, tTG, QD-STV, BT-QD, anti-H-IgA-BT and BSA were prepared in 0.1 M pH 7.4 Tris-HCl buffer (hereafter called Tris buffer).

IMMUNOASSAY PROCEDURES

Biotin detection was carried out following a procedure previously described by our group[1]. Briefly, an aliquot of 10 µL of $1x10^{-7}$ M neutravidin solution (in Tris) was dropped covering completely the working electrode surface. The solution was left overnight at 4 ºC in order to adsorb the protein on the electrode surface. After washing the electrode with Tris buffer, a blocking step was conducted by dropping 40 µL of a BSA solution (2.0% BSA in Tris buffer) and left to adsorb for 30 minutes. After another washing step with Tris, 30 µL of BT and BT-QDs solution (in Tris) was placed on the electrode in order to perform the affinity reaction between neutravidin and BT or BT-QDs. Free BT was only used in the competitive assay. A last washing step was carried out with ultrapure water and the electrode was left to dry and connected to the potentiostat for the voltammetric measurement using differential-pulse anodic stripping voltammetry (DPASV). **Figure S1** shows a schematic drawing of the competitive biosensor.

Detection of anti-tTG IgA antibodies was carried out following a procedure previously described by our group[2]. Briefly, an aliquot of 10 µL of 0.1 mg/mL tTG solution (in Tris) was dropped covering completely the surface of the working electrode. The solution was left overnight at 4 ºC in order to adsorb the protein on the electrode surface. The devices were washed with Tris buffer and 40 µL of a BSA solution (2.0% BSA in Tris buffer) was dropped on the electrode and left to adsorb for 30 minutes in order to avoid non-specific adsorptions, and forming the immunosensor phase. The detection of anti-tTG IgA antibodies was carried out by incubating the immunosensor with 30 µL of serum solutions (1:2 in Tris buffer) for 60 min followed by a washing step with Tris buffer. Then, 40 µL of a 7.5 µg/mL anti-IgA-BT (with 1 mg/mL of BSA) solution were added to the sensor for 60 minutes followed by another washing step with Tris buffer. Finally, 25 µL of QDs-STV (1.5 nM in terms of QDs) were added and left to incubate for 30 minutes. A last washing step was performed with ultrapure water and the electrode was left to dry and connected to the potentiostat for the voltammetric measurement using DPASV. **Figure S2** shows a schematic drawing of the immunosensor following this methodology.

FIGURES

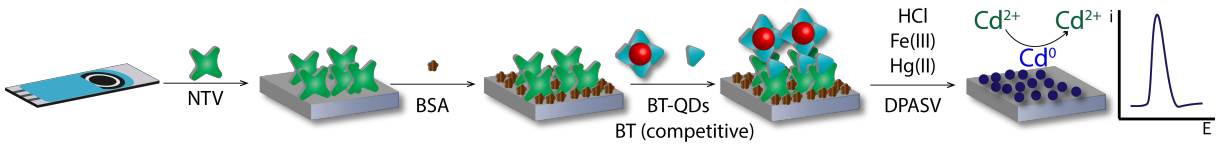

Figure S1. Scheme of the competitive biosensor between neutravidin as recognition element and biotin and biotin labelled with QDs conducted on the surface of screen-printed electrodes. Detection is carried out by ASV in a HCl solution containing Fe(III) and Hg(II).

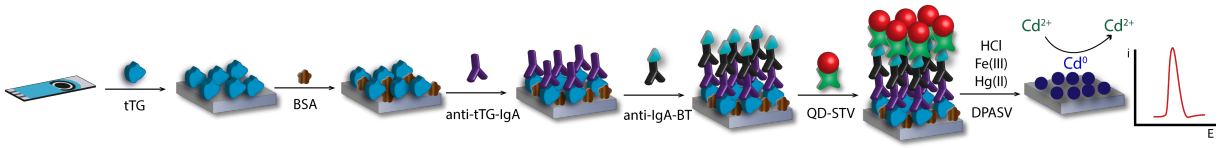

Figure S2. Scheme of the biosensor employed for the detection of anti-transglutaminase IgA antibodies. Tissue-transglutaminase is used as recognition element and the biosensor is carried out on the surface of screen-printed electrodes by incubating in different steps: serum sample, anti-IgA-BT and QDs-STV. Detection is carried out by ASV in a HCl solution containing Fe(III) and Hg(II).

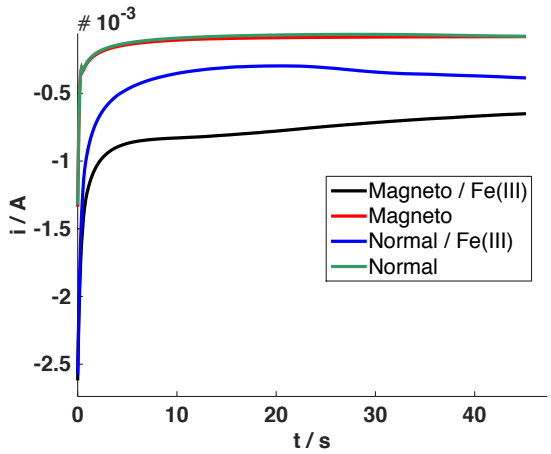

Figure S3. Chronoamperometric responses obtained for the reduction of a solution containing 100 µg/L of Cd(II), 5 mM Hg(II), 0.05 M HCl (optimized conditions) in presence and absence of 50 mM Fe(III) and in absence and presence of a magnetic field. The chronoamperometric current at 20 s was -70 µA in absence of Fe(III) and the magnetic field, -89 µA in absence of Fe(III) and presence of the magnetic field, -298 µA in presence of Fe(III) and absence of the magnetic field and -780 µA in presence of Fe(III) and the magnetic field. The cathodic current is increased in presence of Fe(III) and the magnetic field, and therefore, the Lorentz force will be able to generate a significant convective effect to enhance the mass transfer of cadmium to the electrode surface.

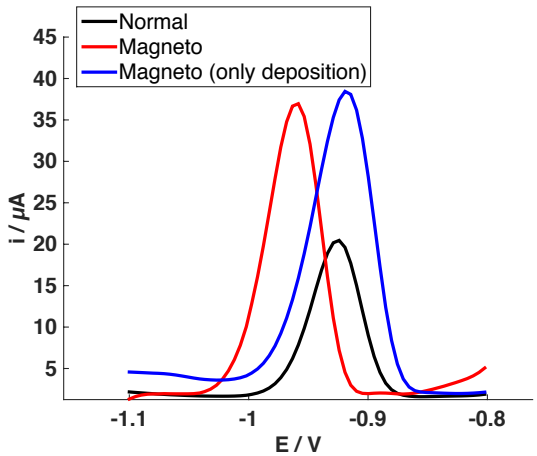

Figure S4. Differential-pulse voltammograms of a solution containing 100 µg/L Cd(II), 0.5 mM Hg(II), 50 mM Fe(III) and 0.05 M HCl (optimized conditions) in absence of the magnetic field (black line), in presence of the magnetic field only in the deposition step (blue line) and in presence of the magnetic field in the deposition and stripping steps (red line). Anodic stripping voltammetry was used in optimized conditions by applying a deposition potential of -1.1 V for 45 s.

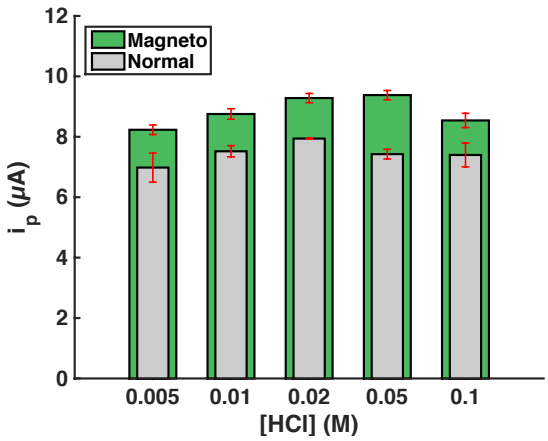

Figure S5. Effect of the HCl concentration on the stripping peak current of 100 µg/L of Cd(II) in presence and absence of a magnetic field. [Hg(II)]: 0.5 mM, [Fe(III)]: 10 mM. Deposition potential and time: -1.1 V for 45 s.

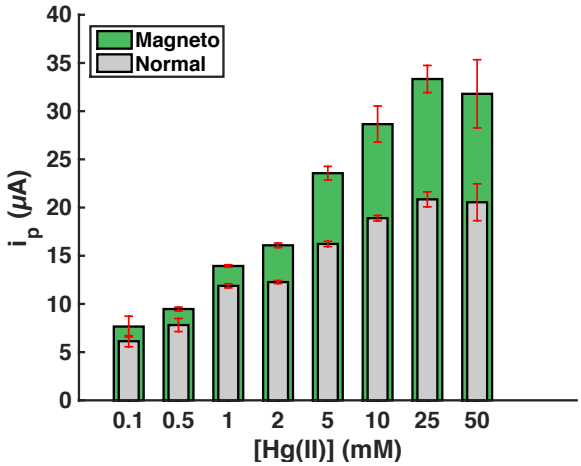

Figure S6. Effect of the Hg(II) concentration on the stripping peak current of 100 µg/L of Cd(II) in presence and absence of a magnetic field. [HCl]: 0.05 M, [Fe(III)]: 10 mM. Deposition potential and time: -1.1 V for 45 s. Although, the peak currents increased up to 25 mM, 5 mM of Hg(II) was chosen due to the potential toxicity of this species.

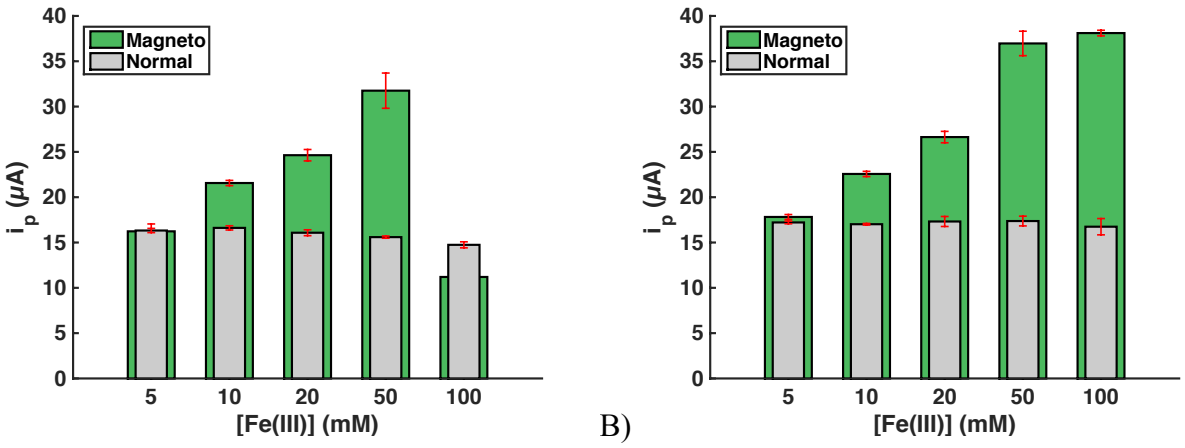

Figure S7. Effect of the Fe(III) concentration on the stripping peak current of 100 µg/L of Cd(II) in presence and absence of a magnetic field. [HCl]: 0.05 M, [Hg(II)]: 5 mM. Deposition potential and time: -1.1 V for 45 s **(A)** and -1.2 V for 45 s **(B)**.

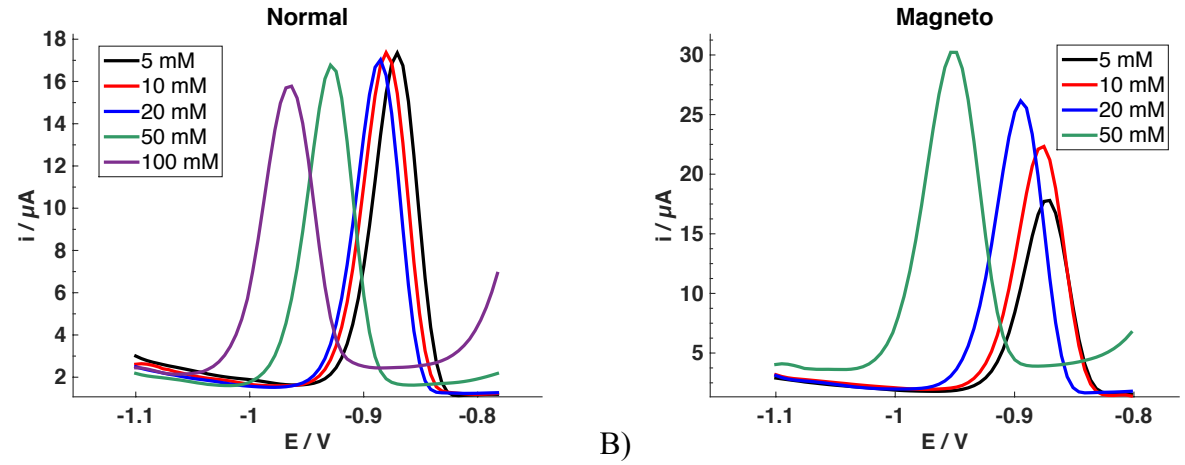

Figure S8. A) Differential-pulse voltammograms of a solution containing 100 µg/L of Cd(II), 5 mM Hg(II) and 0.05 M HCl and different concentrations of Fe(III) (5, 10, 20, 50, 100 mM) in absence of the magnetic field and **B)** in presence of the magnetic field.

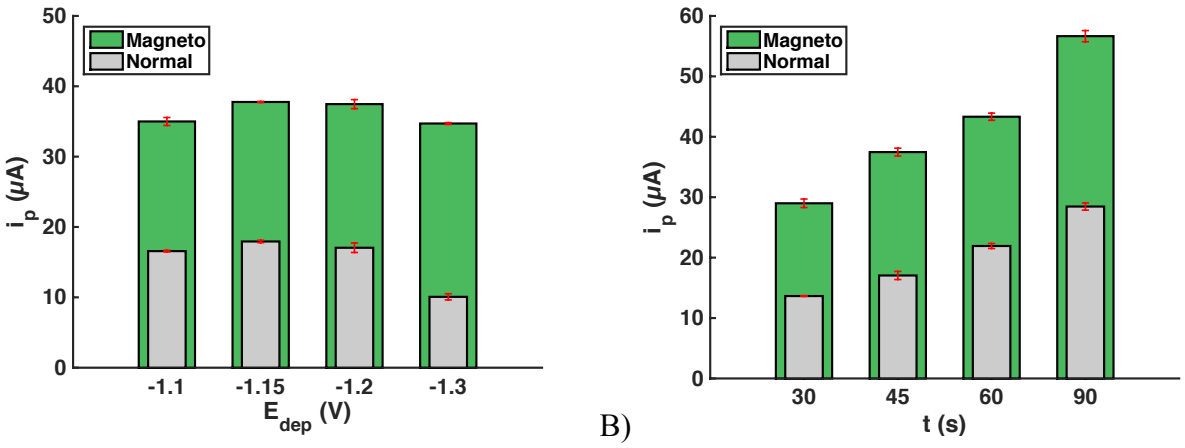

Figure S9. Effect of the deposition potential (E_{dep}) (A) and deposition time (B) on the stripping peak current of a solution containing 100 µg/L Cd(II), 5 mM Hg(II), 50 mM Fe(III) and 0.05 M HCl in presence and absence of a magnetic field. Deposition time in A) was 45 s. Deposition potential in B) was -1.1 V. Although 90 s was chosen as deposition time for the rest of the experiments, higher deposition times could be used in order to achieve a more sensitive detection.

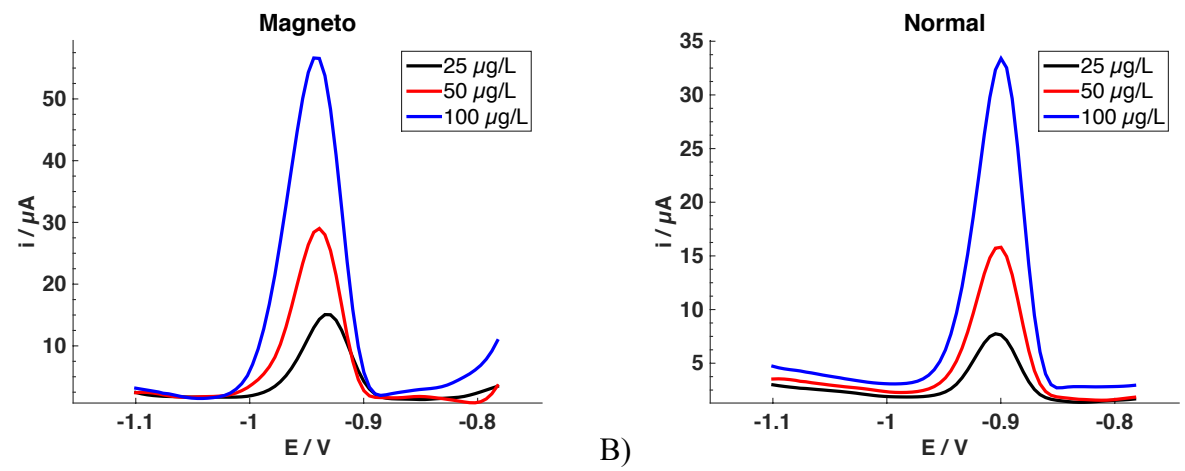

Figure S10. Differential-pulse voltammograms of solutions containing 25 µg/L (black line), 50 µg/L (red line) and 100 µg/L (blue line) of Cd(II), 5 mM Hg(II), 50 mM Fe(III), 0.05 M HCl in absence **(A)** and presence **(B)** of a magnetic field. A deposition potential of -1.1 V was applied for 90 s.

[Cd(II)]		Γ_{ads} (nmol/cm^2)	Deposition efficacy (%)
25 µg/L	Normal	0.13 ± 0.02	15.8
	Magneto	0.26 ± 0.01	17.0
50 µg/L	Normal	0.27 ± 0.02	18.3
	Magneto	0.60 ± 0.02	32.7
100 µg/L	Normal	0.56 ± 0.04	37.8
	Magneto	1.19 ± 0.05	37.3

Table S1. Values found experimentally for the surface coverage (Γ_{ads}) at different Cd(II) concentrations by using anodic stripping voltammetry (deposition: -1.1V, 90s) in presence and absence of the magnetic field. Deposition efficacy is estimated by the ratio between the deposited amount of cadmium and the initial Cd(II) present in solution.

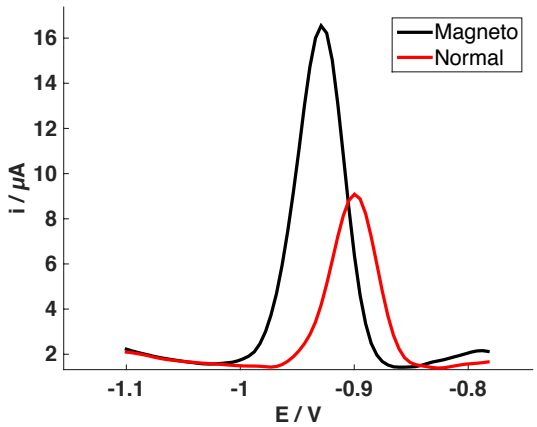

Figure S11. Differential-pulse voltammograms of a solution containing 2 µL of 1 nM QDs (in H_2O) and 45 µL of a solution containing 5 mM Hg(II), 50 mM Fe(III) and 0.05 M HCl in presence (black line) and absence (red line) of a magnetic field.

Reference	Linear range	Sensitivity	LOD
Direct detection[3]	8 - 230 µM	0.05 µA/µM	8 µM
SPCE[4]	~0.1 - 1.25 nM	7 µA/nM	< 0.1 nM
Microfluidic chip (flow)[4]	~0.1 - 1.25 nM	20 µA/nM	< 0.1 nM
Microfluidic device[5]	~0.5 - 7.5 nM	1.4 µA/nM	< 0.5 nM
QDs-HCl[6]	5 - 200 nM	0.23 µA/nM	2.6 nM
Ag@QDs[7]	0.5 - 25 nM	1.57 µA/nM	0.13 nM
This work	0.05 - 5 nM	15.5 µA/nM	0.05 nM

Table S2. Analytical characteristics of several electrochemical methods for the detection of Cd-based quantum dots reported in the literature.

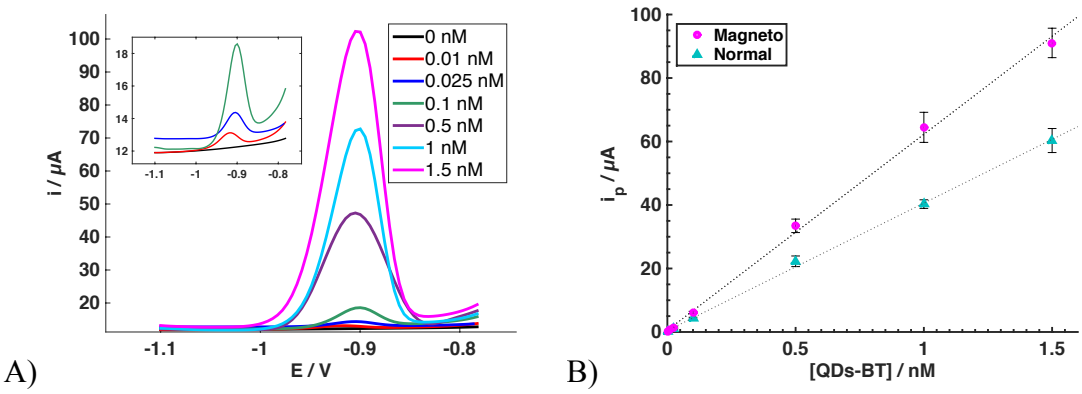

Figure S12. A) Differential-pulse voltammograms for the developed affinity biosensor for the detection of QDs-BT at different concentrations (0, 0.01, 0.025, 0.1, 0.5, 1 and 1.5 nM) in presence of the magnetic field. Inset shows the DPV responses for the lower concentrations of QDs. Procedure of the biosensor is described in section 2.3 of the main manuscript. **B)** Associated calibration plots in presence and absence of the magnetic field.

Reference	LOD (nM)	Linear range (nM)
Avidine-HRP[8]	-	285 - 8000
anti-BT and BT-liposome[9]	14	1 - 1000
MB-STV + HRP-BT[10]	84	94 - 240
MB-STV + HRP-BT (FIA)[11]	0.008	0.01 - 1
MB-STV + HRP-BT (8xSPCEs)[12]	0.2	0.2 - 250
QDs-BT-STV (8xSPCEs)[1]	1.4	1 - 100
This work	0.06	0.16 - 84.5

Table S3. Analytical characteristics of different electrochemical methods for the detection of biotin reported in the literature.

	Expected	Found	Recovery (%)
BT in multivitamin tablet	25 µg	28 ± 2 µg	102 - 115
anti-tTG IgA serum 1	5 U/mL	5.6 ± 0.3 U/mL	108 - 116
anti-tTG IgA serum 2	15 U/mL	14.8 ± 0.5 U/mL	96 - 101
anti-tTG IgA serum 3	30 U/mL	34 ± 3 U/mL	108 - 121
anti-tTG IgA positive control	26 ± 7 U/mL	27 ± 1 U/mL	-
anti-tTG IgA negative control	< 3 U/mL	1.7 ± 0.4 U/mL	-

Table S4. Values of concentration (or amount) expected for the real samples evaluated and the concentration determined experimentally by using the biosensors developed in presence of the magnetic field.

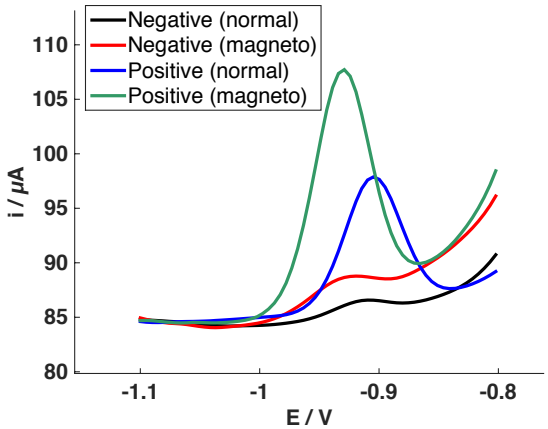

Figure S13. Differential-pulse voltammetry for the detection of anti-tTG IgA antibodies using the positive and negative serum controls in presence and absence of the magnetic field.

References

(1) Martín-Yerga, D.; González-García, M. B.; Costa-García, A. *Sens. Actuators B* **2013**, *182*, 184–189.

(2) Martín-Yerga, D.; Costa-García, A. *Bioelectrochemistry* **2015**, *105*, 88–94.

(3) Merkoçi, A.; Marcolino-Junior, L. H.; Marín, S.; Fatibello-Filho, O.; Alegret, S. *Nanotechnology* **2007**, *18* (3), 35502.

(4) Medina-Sánchez, M.; Miserere, S.; Cadevall, M.; Merkoçi, A. *Electrophoresis* **2016**, *37* (3), 432–437.

(5) Medina-Sánchez, M.; Miserere, S.; Morales-Narváez, E.; Merkoçi, A. *Biosens. Bioelectron.* **2014**, *54*, 279–284.

(6) Martín-Yerga, D.; Bouzas-Ramos, D.; Menéndez-Miranda, M.; Bustos, A. R. M.; Encinar, J. R.; Costa-Fernández, J. M.; Sanz-Medel, A.; Costa-García, A. *Electrochim. Acta* **2015**, *166*, 100–106.

(7) Martín-Yerga, D.; Rama, E. C.; Costa-García, A. *Anal. Chem.* **2016**, *88* (7), 3739–3746.

(8) Wright, J. D.; Rawson, K. M.; Ho, W. O.; Athey, D.; McNeil, C. J. *Biosens. Bioelectron.* **1995**, *10* (5), 495–500.

(9) Ho, J. A.; Hsu, W.-L.; Liao, W.-C.; Chiu, J.-K.; Chen, M.-L.; Chang, H.-C.; Li, C.-C. *Biosens. Bioelectron.* **2010**, *26* (3), 1021–1027.

(10) Kergaravat, S. V.; Gómez, G. A.; Fabiano, S. N.; Laube Chávez, T. I.; Pividori, M. I.; Hernández, S. R. *Talanta* **2012**, *97*, 484–490.

(11) Biscay, J.; González García, M. B.; Costa García, A. *Talanta* **2015**, *131*, 706–711.

(12) Biscay, J.; García, M. B. G.; García, A. C. *Sens. Actuators B* **2014**, *205*, 426–432.